Decimated Signal Diagonalization for Fourier Transform Spectroscopy

Dž. Belkić,[†,||] P. A. Dando,[†] J. Main,[‡] H. S. Taylor,[*,†] and S. K. Shin[§,⊥]

Department of Chemistry, University of Southern California, Los Angeles, California 90089-0482, USA, Department of Medical Radiation Physics, Karolinska Institute, P.O. Box 260, S-17176, Stockholm Sweden, Institut für Theoretische Physik und Synergetik, Universität Stuttgart, D-70550 Stuttgart, Germany, and Department of Chemistry, University of California, Santa Barbara, California 93106-9510, USA

Received: April 26, 2000; In Final Form: September 8, 2000

A nonlinear parameter estimator with frequency-windowing for signal processing, called Decimated Signal Diagonalization (DSD), is presented. This method is used to analyze exponentially damped time signals of arbitrary length corresponding to spectra that are sums of pure Lorentzians. Such time signals typically arise in many experimental measurements, e.g., ion cyclotron resonance (ICR), nuclear magnetic resonance or Fourier transform infrared spectroscopy, etc. The results are compared with the standard spectral estimator, the Fast Fourier Transform (FFT). It is shown that the needed absorption spectra can be constructed simply, without any supplementary experimental work or concern about the phase problems that are known to plague FFT. Using a synthesized signal with known parameters, as well as experimentally measured ICR time signals, excellent results are obtained by DSD with significantly shorter acquisition time than that which is needed with FFT. Moreover, for the same signal length, DSD is demonstrated to exhibit a better resolving power than FFT.

1. Introduction

Recently, we have introduced a new method, termed Decimated Signal Diagonalization (DSD), for obtaining the complete eigenspectra of arbitrarily large matrices that are theoretically generated with auto-correlation functions from time propagated wave packets.[1] Using the previously established equivalence between the auto-correlation functions and the exponentially damped signals corresponding to spectra that are sums of pure Lorentzians,[2,3] this paper extends DSD to signal processing. Many experimental time signals, such as those arising from ion cyclotron resonance (ICR), nuclear magnetic resonance (NMR), Fourier transform infrared (FTIR) spectroscopy, and so forth, are of this latter form.[4,5] Although DSD can be used to analyze any such signal, the examples presented here concentrate on time signals obtained from ICR experiments.

The DSD of ref 1 relies upon the part of the Wall−Neuhauser[2] Filter Diagonalization (FD) method, in the Mandelshtam−Taylor[3] discrete version, which uses the signal to create the matrixes of a generalized eigenvalue problem. Upon diagonalization, this yields the spectral parameters of the desired Lorentzian spectrum. The common key to the success of both FD and DSD is the introduction of windowing techniques with the purpose of significantly reducing the large dimensions of the matrices that need to be diagonalized. Without this reduction, any diagonalization procedure, even with the use of regularization techniques such as singular value decomposition (SVD) and the like, becomes numerically unstable for large matrices and often yields spurious peaks. This problem can be traced back to the fact that the rank of the matrices, i.e., the number of spectral Lorentzians, is usually much smaller than their dimension, which is half the length of the signal.

As seen below, windowing in DSD is performed prior to the introduction of any signal processing model. The band-limited decimation as a particular windowing employed here is, in fact, a generic procedure because it is not necessarily limited to diagonalization methods for signal processing. As such, the shortened beamspace-windowed signal can be subjected to other processors as originally pointed out in ref 1 and recently illustrated in refs 6 and 7. In Section 2 of the present paper, we outline the theory and comment on several advantageous features of DSD. Of particular importance is that, for a given signal length, DSD has a better resolving power than FFT. As a result, DSD usually achieves convergence with a significantly shorter acquisition time than needed with FFT. Although the measurement of long time signals presents few difficulties experimentally, there is a distinct advantage to be gained by using shorter signals. The exponential decay of the signal amplitude with time means that longer time signals can become overwhelmed by noise. Eventually, the noise obscures the very signal structure whose resolution demands the longer acquisition time. DSD avoids this problem to an extent by achieving resolution before reaching a signal length where noise becomes too significant. This important point is demonstrated in Section 3, in which we give the test examples for a synthesized model signal with known peak parameters, as well as for three experimentally measured ICR time signals. The conclusion is in Section 4.

2. Theory

In this section, we describe the DSD as a parameter estimator for the processing of time signals such as the ones that arise typically in Fourier transform-based spectroscopic experiments. Central to the success of the DSD method is the introduction of a windowing technique called "band-limited decimation", which is different from that implemented in FD.[2,3]

* To whom correspondence should be addressed.
† Department of Chemistry, University of Southern California.
|| Department of Medical Radiation Physics, Karolinska Institute.
‡ Institut für Theoretische Physik und Synergetik, Universität Stuttgart.
§ Department of Chemistry, University of California.
⊥ Present address: Department of Chemistry, Pohang University of Science and Technology, San 31 Hyojadong Nam-Gu, Pohang, Kyungbuk, Korea, 790-784..

10.1021/jp0015933 CCC: $19.00
Published on Web 11/18/2000

2.1. Windowing. The windowing procedure used in DSD is simple and can be briefly explained as follows. We start with the digitized time signal $\{c_n\}$ $(0 \le n \le N-1)$ which consists of N points, equidistantly sampled with a "dwell" time τ and having a total bandwidth of $2\pi/\tau$. To initialize windowing, $\{c_n\}$ is subjected to a discrete Fourier transform using the efficient FFT algorithm to obtain the Fourier spectrum

$$F_k = \sum_{n=0}^{N-1} c_n\, e^{2\pi i k n/N},\ (k = 0, ..., N-1) \qquad (1)$$

which is accurate only at the Fourier grid points, k, corresponding to the frequencies $\omega_k = 2\pi k/(N\tau)$. In general, the FFT of eq 1 yields what turns out to be, relative to the final spectrum, a low-resolution spectrum as the number of signal points, N, will be insufficient for the FFT to resolve dense eigenfrequencies.

Next, the frequency window of interest, $\omega \in [\omega_{k_{\min}}, \omega_{k_{\max}}]$, is chosen. To reduce the ill-conditioning of the subsequent processing, the number of Fourier grid points, $N_D = k_{\max} - k_{\min} + 1$, contained in the window should not exceed more than about 200. The N_D elements, F_k, of the low resolution Fourier spectrum located within the window are then selected and shifted to reposition them symmetrically about the frequency origin, $\omega = 0$. That is, the central frequency of the window, $\omega_0 = 2\pi k_0/(N\tau)$ where $2k_0 = k_{\max} + k_{\min}$, is subtracted from every frequency ω belonging to the actual window. In this way, the band-limited decimated FFT spectrum, $\{F_k^{\mathrm{bld}}\}$ $(0 \le k \le N_D - 1)$, is created. Specifically, we have $F_{k-k_0}^{\mathrm{bld}}$ for $k_{\min} \le k \le k_{\max}$ with the periodicity of the FFT used to identify $F_j^{\mathrm{bld}} = F_{N_D+j}^{\mathrm{bld}}$ when $j < 0$. The result is a spectrum centered at $\omega = 0$ with a bandwidth of $2\pi N_D/(N\tau)$.

Finally, an inverse FFT is applied to $\{F_k^{\mathrm{bld}}\}$ to obtain the so-called "band-limited decimated" (bld) signal $\{c_n^{\mathrm{bld}}\}$ $(0 \le n \le N_D - 1)$ of shorter length N_D, which is valid for the window of interest. The new bandwidth is reduced $M = N/N_D$ times from that of the original signal. Hence, the dwell time of the band-limited decimated signal is now augmented by M so that $\tau_D = M\tau$ giving the same total acquisition time as used for c_n, i.e., $T = N\tau = N_D\tau_D$. By employing the band-limited decimated signal, the problem is reduced to one of signal processing a significantly shortened effective signal. The key steps in the creation of the band-limited decimated signal are shown schematically in Figure 1.

To scan the whole bandwidth of the original signal $[-\pi/\tau, +\pi/\tau]$, we must form the Fourier spectra $\{F_k^{\mathrm{bld}}\}$ and the resulting band-limited decimated signal $\{c_n^{\mathrm{bld}}\}$ separately for each of M windows. Note, however, that the first FFT of the original signal of length N is common to each of the M windows and hence need be performed only once. In any case, none of this preprocessing is computationally intensive as each FFT scales with the signal length as $N \log_2 N$. Relative to diagonalization, the CPU time required for the windowing is negligible.

In any of the windows, $[\omega_{\min}, \omega_{\max}]$, the resulting FFT spectra $\{F_k^{\mathrm{bld}}\}$ created from $\{c_n^{\mathrm{bld}}\}$ are, by construction, identical (apart from the centering of the spectrum about ω_0) to the corresponding Fourier spectra $\{F_k\}$ based solely upon $\{c_n\}$. This establishes the key feature of the procedure, which is that the information content in each of the M individual windows is preserved in the process of band-limited decimation. We emphasize this crucial feature of the *band-limited decimation* to avoid any potential confusion with a *straightforward decimation*, which always leads to a loss of information. Some distortion of the bld signal can occur for very narrow windows, and caution must be exercized when using DSD for such windows that contain a small number of Fourier grid points (i.e., small N_D).

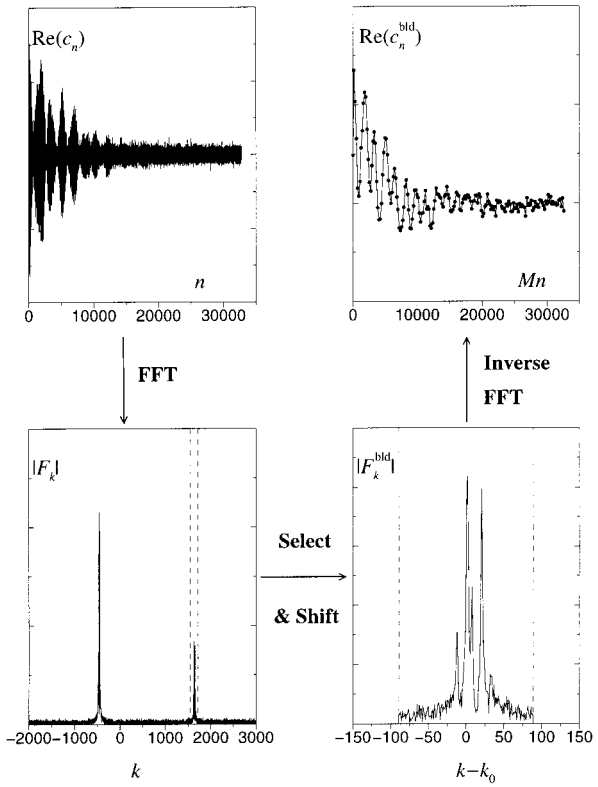

Figure 1. Schematic of the band-limited decimation process. The original signal (for clarity, only the real part of the signal is shown in the upper left-hand panel) is first subjected to the FFT, yielding the low resolution spectrum a small part of which is shown in the lower left-hand panel. Next, a small window is chosen as indicated by the dashed vertical lines. The values of the F_k elements within the window are shifted in frequency so that the window is symmetric about $k = 0$ to give the band-limited Fourier spectrum, F_k^{bld} (bottom right-hand panel). An inverse FFT is then applied to obtain the real and imaginary parts of the band-limited decimated signal points, c_n^{bld}. In the upper right-hand panel, the real part of the resulting c_n^{bld} are marked by the filled circles and the full lines are drawn to guide the eye. The imaginary part of c_n^{bld} (not shown) exhibits a similar behavior. Note that we plot Re(c_n^{bld}) against Mn to emphasize that the acquisition time of the c_n^{bld} is identical to that of the original signal shown in the upper left-hand panel.

In our numerical implementation of band-limited decimation, we explicitly use the robust numerical routines for FFT and inverse FFT to take full advantage of the mentioned quasi-linear scaling with the increasing signal length. Note, however, that the prescription outlined permits a straightforward derivation of the following analytical formula

$$c_n^{\mathrm{bld}} = \frac{1}{N} \sum_{n'=0}^{N-1} c_{n'} e^{2\pi i n' k_0/N} \frac{\sin(\pi[n/N_D - n'/N])}{(\pi[n/N_D - n'/N])} \qquad (2)$$

with $0 \le n \le N_D - 1$. It is clear from here that band-limited decimation *always uses the whole set* $\{c_{n'}\}$ $(0 \le n' \le N-1)$ of the original signal in constructing the new sequence $\{c_n^{\mathrm{bld}}\}$. In other words, the only trace of band-limited decimation in $\{c_n^{\mathrm{bld}}\}$ is in a weight function, given by the complex phase modulated ratio of the two sinusoids in eq 2. A crucial consequence of such a structure in eq 2 is that no original signal point $c_{n'}$ is ever dropped from $\{c_n^{\mathrm{bld}}\}$. This does not necessarily imply that the whole set $\{c_{n'}\}$ $(0 \le n' \le N-1)$ must always

be exhausted for every application in practice. As a matter of fact, it will be shown in Section 3 that DSD with $\{c_n^{\mathrm{bld}}\}$ can successfully complete the full spectral analysis by using only a fraction (sometimes one-quarter) of the length N of the original signal $\{c_{n'}\}$.

2.2. Decimated Signal Diagonalization. We now describe the diagonalization procedure that extracts all of the relevant peak parameters, namely the complex frequencies and amplitudes, $\{\omega_k, d_k\}$, from the window $[\omega_{\min}, \omega_{\max}]$. As with FD, the DSD technique is restricted to signals that are given as sums of damped exponentials. Therefore, we model the band-limited decimated signal c_n^{bld} as

$$c_n^{\mathrm{bld}} = \sum_{k=1}^{K} d_k e^{-i\omega_k n\tau_D}, \quad \mathrm{Im}\ \omega_k < 0 \tag{3}$$

where the condition Im $\omega_k < 0$ selects only those physically meaningful harmonics that decay exponentially with increasing time and K is the so-called local spectral rank which is equal to the number of Lorentzians generated by eq 3. Here, the order/rank K need not be finite/fixed or even known prior to the analysis, in contrast to the initial condition of, e.g., one of the most frequently used methods in ICR and NMR known as the Linear Predictor (LP).[6] By comparison, the inverse Fourier transform, $c_n = \sum_{k=0}^{N-1} F_k e^{-2\pi ikn/N}$, from eq 1 also appears as a sum of exponentials with the complex amplitudes $\{d_k\}$ given by $\{F_k\}$. However, unlike eq 3, these latter exponentials are undamped, and their purely real frequencies $\{\omega_k\}$ are *pre-fixed* at the Fourier grid points, $\omega_k\tau = 2\pi k/N$. Consequently, the FFT and inverse FFT represent linear mappings as opposed to the nonlinear ansatz in eq 3, where both d_k and ω_k are the fitting parameters. It is *this* fact that furnishes a possibility to improve frequency resolution by all the spectral estimators that use nonlinear fits for c_n or c_n^{bld} as modeled by eq 3.

The method upon which the DSD relies for converting the nonlinear fit of eq 3 into an equivalent diagonalization problem was first devised by Wall and Neuhauser[2] and later reformulated by Mandelshtam and Taylor[3] for the processing of time signals defined on evenly spaced discrete time grids. The details of such a conversion within FD can be found in refs 2 and 3, and therefore, only a brief outline suffices for an equivalent procedure within DSD. The crucial idea is to associate the complex signal points, c_n^{bld}, to be modeled by the form of eq 3, with a discrete time auto-correlation function

$$C_n^{\mathrm{bld}} = (\Phi_0|\hat{U}(n\tau_D)\Phi_0) \tag{4}$$

generated by the time evolution operator $\hat{U}(\tau_D) = \exp(-i\hat{\Omega}\tau_D)$ of a "fictitious" dynamical system with an effective complex symmetric "Hamiltonian" operator, $\hat{\Omega}$. In eq 4, Φ_0 represents some "initial" state of the system and a complex symmetric inner product $(a|b) = (b|a)$, i.e., without complex conjugation, is used. Note that neither the operator $\hat{U}$ (or, equivalently, $\hat{\Omega}$) nor Φ_0 need be known or given explicitly. It is further supposed that there exists an orthonormal set of eigenvectors $\{\mathrm{Y}_k\}$ that diagonalizes the evolution operator. Then we can write

$$\hat{U} = \sum_k |\mathrm{Y}_k)u_k(\mathrm{Y}_k| = \sum_k e^{-i\tau_D\omega_k}|\mathrm{Y}_k)(\mathrm{Y}_k| \tag{5}$$

where $u_k = \exp(-i\tau_D\omega_k)$ are the eigenvalues of $\hat{U}$. Substitution of eq 5 into eq 4, followed by the identification

$$d_k = (\Phi_0|\mathrm{Y}_k)(\mathrm{Y}_k|\mathrm{Y}_0) = (\mathrm{Y}_k|\mathrm{Y}_0)^2 \tag{6}$$

leads directly to the right-hand side of eq 3 and, therefore, $C_n^{\mathrm{bld}} = c_n^{\mathrm{bld}}$. Hence, the eigenvalues of $\hat{U}$ determine the complex frequencies ω_k via $u_k = \exp(-i\omega_k\tau_D)$, whereas the corresponding eigenvectors give the complex amplitudes, d_k, from eq 6. In other words, diagonalization of $\hat{U}$ yields all the desired parameters, $\{\omega_k, d_k\}$.

Although $\hat{U}$ may not be known explicitly, its matrix elements in an appropriately chosen basis are always determined completely by the $\{c_n^{\mathrm{bld}}\}$. The simplest available basis is that consisting of the primitive Krylov vectors $\{\Phi_n\}$ generated by the evolution operator

$$|\Phi_n) = \hat{U}^n|\Phi_0) = e^{-in\tau_D\hat{\Omega}}|\Phi_0),\ n = 0, ..., K-1 \tag{7}$$

where $K = [N_D/2]$ with $[\alpha]$ denoting the integer part of α.

When expressed in terms of the Krylov basis, all the matrix elements of $\hat{U}$ depend only on the set $\{c_n^{\mathrm{bld}}\}$ through the remarkably simple prescription[3]

$$U_{nm} = (\Phi_n|\hat{U}\Phi_m) = (\Phi_n|\Phi_{m+1}) = c_{n+m+1}^{\mathrm{bld}} \tag{8}$$

Because the basis is not orthonormal, the overlap matrix $\mathbf{S} = \{S_{nm}\}$ is also needed and this is given by[3]

$$S_{nm} = (\Phi_n|\Phi_m) = (\hat{U}^n\Phi_0|\hat{U}^m\Phi_0) = (\Phi_0|\hat{U}^{m+n}\Phi_0) = c_{m+n}^{\mathrm{bld}} \tag{9}$$

which again is related trivially to the set $\{c_n^{\mathrm{bld}}\}$. Of course, relations (8) and (9) are entirely similar to those first encountered in FD, with the exception that DSD uses the band-limited decimated signal points $\{c_n^{\mathrm{bld}}\}$ rather than the original ones $\{c_n\}$. Clearly eqs 8 and 9 render DSD independent of the measured or computational origin of the decaying time signals of the form of eq 3.

With the above-described ansatz (4) and the mentioned equivalence $C_n^{\mathrm{bld}} = c_n^{\mathrm{bld}}$, the nonlinear fitting in eq 3 is converted in DSD into a linear algebra equation through solving an equivalent generalized eigenvalue problem,[2,3]

$$\boldsymbol{U}\boldsymbol{B}_k = u_k\boldsymbol{S}\boldsymbol{B}_k \tag{10}$$

for the eigenvalues $u_k = \exp(-i\omega_k\tau_D)$ of the operator $\hat{U} = [\exp(-i\hat{\Omega}\tau_D)]$ with the elements of the $K \times K$ matrices $\boldsymbol{U}$ and $\boldsymbol{S}$ given by eqs 8 and 9, respectively. The column vectors $\boldsymbol{B}_k$ with elements B_{nk} are normalized with respect to the overlap matrix $\boldsymbol{S}$, i.e.,

$$\boldsymbol{B}_j^T\boldsymbol{S}\boldsymbol{B}_k = \delta_{jk} \tag{11}$$

and define the eigenvectors Y_k in terms of the *locally* complete Krylov basis functions Φ_n as

$$\mathrm{Y}_k = \sum_{n=0}^{K-1} B_{nk}\Phi_n \tag{12}$$

Substituting eq 12 into eq 6 gives

$$d_k = \Big(\sum_{n=0}^{K-1} B_{nk}c_n^{\mathrm{bld}}\Big)^2 \tag{13}$$

which provides an explicit, closed form expression which can be used to compute the complex amplitudes $\{d_k\}$.

The DSD now diagonalizes eq 10 to determine all the peak parameters $\{\omega_k, d_k\}$ in the window $[\omega_{\min}, \omega_{\max}]$ and then

constructs a *local* spectrum in any mode, e.g., magnitude $|F(\omega)|$, power $|F(\omega)|^2$ and, most importantly, absorption $A(\omega)$. This is performed at an *arbitrary* real frequency ω from the chosen window through the following sum of complex Lorentzians

$$F(\omega) = -i\sum_{k=1}^{K} \frac{d_k}{\omega - \omega_0 - \omega_k} \tag{14}$$

which is obtained simply by taking the Fourier integral of eq 3 in the continuous time limit. The real central frequency $\omega_0 = (\omega_{\min} + \omega_{\max})/2$ of the window $[\omega_{\min}, \omega_{\max}]$ is added to every complex resonance ω_k to compensate for the shift to the origin $\omega = 0$ of the band-limited Fourier spectrum F_k^{bld} invoked in construction of each c_n^{bld}. To compute an a priori positive definite absorption spectrum, $A(\omega) \geq 0$, at any real ω we propose the formula

$$A(\omega) = \sum_{k=1}^{K} |d_k| \frac{-\text{Im}\ \omega_k}{(\omega - \omega_0 - \text{Re}\omega_k)^2 + (\text{Im}\ \omega_k)^2} \tag{15}$$

This follows from eq 14 by requiring that $\text{Re}\{F(\omega)\}$ and $\text{Im}\{F(\omega)\}$ are purely absorptive and dispersive spectrum, respectively. Unlike the complex spectrum $F(\omega)$ from eq 14, the absorption mode $A(\omega)$ in eq 15 has no interference effects, due to the deliberate omission of the signal phase $\text{Arg}(d_k)$ in $|d_k| = |d_k e^{i\ \text{Arg}(d_k)}|$. The diagonalization generally yields both physical ($\text{Im}\ \omega_k < 0$) and spurious ($\text{Im}\ \omega_k > 0$) eigenfrequencies. The latter ones have been retained in the final spectra previously calculated in FD[3] by using one of the several existing reflections, e.g., $\text{Im}\ \omega_k \rightarrow -|\text{Im}\ \omega_k|$, and so forth. A similar procedure could also be employed in DSD. We emphasize again that DSD is limited only to Lorentzian spectra that in the time domain are modeled by sums of damped exponentials (3).

The ability to obtain an absorption spectrum with its enhanced resolution and, due to the lack of interference between Lorentzian peaks, its clearer appearance is an advantage of DSD over the standard FFT. As mentioned before, the FFT sequence $\{F_k\}$ coincides with the set of the complex amplitudes $\{d_k\}$ in the original signal c_n which can be conceived as the inverse FFT, F_k^{-1}. Here, the correct phase $\text{Arg}(d_k)$ of d_k must be known before the set $\{F_k\}$ could be decomposed into its absorption and dispersion parts, $A(\omega)$ and $D(\omega)$, by using the "single line" prescription, $e^{-i\ \text{Arg}(d_k)}\ F(\omega) = A(\omega) + iD(\omega)$, which is correct only at the Fourier grid points, $\omega\tau = 2\pi k/N$. Obtaining the proper phase in FFT is nontrivial, as often a subset of early signal points from the sequence $\{c_n\}$ may not be collected for reasons of experimental difficulties. Therefore, the resulting $\{d_k\}$ could have an incorrect phase. To remedy this in, e.g., NMR experiments, certain empirical corrections can be made because the length of the missing front part of the signal is usually short. However, this is often not the case in typical ICR measurements and true absorption spectra are virtually impossible to obtain. Here, both resolution and transparency of the spectra are sacrificed by displaying the magnitude $|F(\omega)|$ of $F(\omega)$ which includes the dispersion contribution, $D(\omega)$. This latter term dies off too slowly as $\sim 1/\omega$ with the frequency separation from $\text{Re}(\omega_k)$ and, therefore, causes an overall poor resolution and/or performance of FFT. The process of taking the magnitude of the complex function $F(\omega)$ leads to the interference which is only worse due to the enhanced overlay of lines. In any of the harmonic inversion methods of which DSD is only one example, the complex $\{d_k\}$ and the complex $\{\omega_k\}$ are the fitting parameters that constitute the so-called "line list", which is determined prior to constructing a spectrum and *this* facilitates emergence of an absorption mode (15). In principle, there is no need to go beyond the line list which contains all the required information. We say "in principle" because the ubiquitous noise in the signal, which can hardly satisfy the forms such as eq 3, causes the appearance of many spurious entries in the line list. It then seems appealing to visually inspect the obtained spectra with the intention of roughly disentangling noise from signal as a first approximation to a more comprehensive noise reduction technique (for a more detailed discussion, see, e.g., ref 6).

If required, all the above-outlined steps in DSD can be repeated M times to scan the frequency window $[\omega_{\min}, \omega_{\max}]$ throughout the whole Nyquist interval. In so doing, the signal length N_{D} may be allowed to vary from window to window. It is tempting to think that, when connecting together these partial spectra, the sharp rectangular window employed could lead to some phase distortions at the edges of the adjacent windows. This is the so-called "aliasing" which exists for general signals, but *not* for the band-limited ones, such as, e.g., $\{c_n^{\text{bld}}\}$. The present procedure of band-limited decimation belongs to a broader class of the well-known "anti-aliasing" filters. Should a larger portion of a spectrum and/or the whole Nyquist interval be analyzed by DSD, a significant overlap of the neighboring windows is recommended. This should be followed subsequently by discarding the narrow edges of each of the local spectra (see Section 3, example 3).

For comparison, windowing in FD is accomplished using a linear combination of the primitive Krylov basis functions (7) with the Fourier coefficients, but keeping the original signal c_n throughout. Such a windowing also secures emergence of the diagonally dominated elements in the matrix $\boldsymbol{U}$. This dimensionality reduction of the original problem is performed during diagonalization and, as such, is limited exclusively to FD. By contrast, our windowing procedure is carried out directly on the original time domain data c_n and is, therefore, completely dissociated from the spectral analysis, so that the band-limited signal c_n^{bld} can be subjected to any of the existing processors.

The above-achieved dimensionality reduction of the matrix $\boldsymbol{U}$ does not, of course, eliminate the inherent ill-conditioning problem in eq 3 for the underlying harmonic inversion. Rather, the round-off error problems become controllable and non-accumulative, so that certain routine procedures, e.g., singular value decomposition (SVD), Householder's or Cholesky's decomposition or the QZ algorithm, as implemented in, e.g., the NAG Library,[8] lead to stable algorithms producing accurate results.

Overall performance of DSD is deemed accurate, stable, and robust as our concrete computations combined with thorough testing have indeed confirmed. The robustness of DSD stems from the way it performs the windowing. Here, the two robust processors, FFT and inverse FFT, effectively prepare all the matrix elements U_{nm} and S_{nm} as seen in eqs 8 and 9, respectively.

As with several other parameter estimators, DSD exhibits an advantage over FFT in resolving power. For example, DSD has the same resolution as FFT for shorter acquisition time, or equivalently higher resolution for the same signal length. This can be seen from the respective uncertainty principles, $N_{\text{FFT}} \propto 2\pi/(\tau\Delta\omega_{\min})$, for FFT and $N_{\text{DSD}} \propto 4\pi/(\tau\Delta\omega_{\text{av}})$, for DSD where $\Delta\omega_{\min}$ and $\Delta\omega_{\text{av}}$ are the minimum and average spacings between eigenvalues in the given window, respectively. Because generally $\Delta\omega_{\text{av}} > \Delta\omega_{\min}$, we have $N_{\text{DSD}} < N_{\text{FFT}}$.

As opposed to DSD, which is a parameter estimator, FFT is a spectral estimator, which can directly provide only the shape

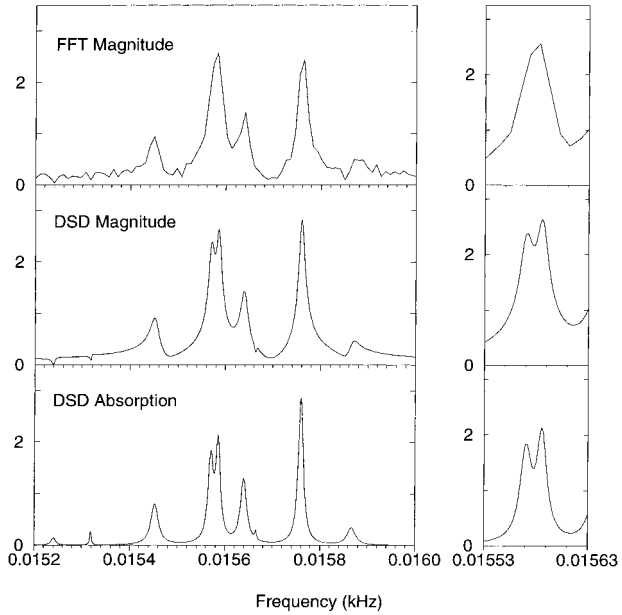

Figure 2. Spectra for a "noisy" synthesized time signal consisting of a sum of exponentially damped oscillations with known amplitudes, phases, and damping constants. Gaussian distributed zero-mean random noise of standard deviation 0.5 is added to the signal to simulate a noise contamination of roughly 30%. The three panels on the right-hand side show magnifications of the doublet located at 0.015 570−0.015 585 kHz.

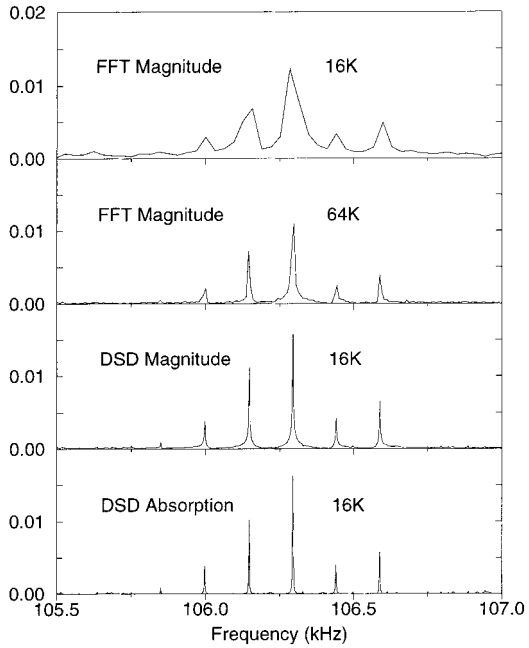

Figure 3. ICR frequency spectra of singly charged molecular ions $[C_{59}N]^+$ and $[C_{60}]^+$. The time signal was obtained via a single time-domain data acquisition using the Matrix Assisted Laser Desorption Ionization (MALDI). Employing merely one-quarter of the full signal length, DSD obtains the entire elemental structure with the correct relative abundance of all the isotopes. The largest peak in the spectrum is associated with the monoisotopic $[^{12}C_{59}{}^{14}N]^+$ ion.

of a spectrum. To obtain the resonance parameters from a given FFT spectrum, one customarily resorts to a Lorentzian-type fitting as in eq 3 for each peak, but this time via nonlinear least-squares minimizations. In most cases, this is insufficiently accurate and does not work well with overlapping Lorentzians. Due to nonlinear fitting, one must first estimate initial values of the unknown $\{\omega_k, d_k\}$ and poor guesses might lead to severe deviations from the expected, true results. This approach becomes particularly impractical for dense spectra with a large number of peaks. All of these difficulties are absent from DSD, which finds the required peak parameters $\{\omega_k, d_k\}$ directly by solving eq 10.

3. Examples

Here, we display and briefly discuss the results obtained for the performed tests of DSD in both the case of a theoretically synthesized model signal of the form given in eq 3 with known complex peak parameters $\{\omega_k, d_k\}$ (Figure 2) and the case of experimentally measured ICR time signals (Figures 3, 4 and 5). The DSD is applicable to any time signal modeled by sums of attenuated complex exponentials with constant amplitudes as customarily encountered in most ICR, NMR, or FTIR experiments. The simulated model problem is selected in such a way that the given peak parameters $\{\omega_k, d_k\}$ could realistically mimic some typical time signals recorded in these experiments. Conversely, both groups of the illustrations, the synthesized and the experimental signals, are deemed sufficiently general, representative, and challenging to provide a reliable test for assessing the validity and usefulness of the DSD with respect to the FFT. With this main purpose of the present testing, we will briefly explain the experimental samples without going into details of their specific relevance for the ICR community, as such information is readily available in the references in which these signals and their FFT spectra have been originally reported.

As a first test we used FFT and DSD to obtain the spectra of a simulated time signal of the form of eq 3. The signal consisted of 54 known complex peak parameters, $\{\omega_k, d_k\}$, with $\mathrm{Re}(\omega_k)$ distributed throughout the total bandwidth of 312.5 Hz. A total of $N = 32$ K signal points were computed with a dwell-time of $\tau = 3.2$ milliseconds. The standard deviation of the resulting signal was $\sigma = (\sum_{n=0}^{N-1}|c_n|^2/N)^{1/2} = 1.652$. Finally, Gaussian distributed white noise with zero mean and standard deviation $\sigma = 0.5$ was added to the signal to simulate a noise contamination of roughly 30%. This final "noisy" signal can be regarded as typical of time signals that would be measured, for example, in a high-resolution ICR experiment.

Analysis of this synthesized signal with 30% noise produces the FFT and DSD spectra shown in Figure 2. For clarity, we show only a small frequency window in the region 0.015−0.016 kHz. The superior frequency resolving power of DSD is clear. In contrast to FFT, the present method separates the close doublet at 0.015 570−0.015 585 kHz which is further magnified in the panels on the right-hand side of Figure 2. In addition, the small peak at 0.01587 kHz is almost completely masked by noise in the FFT and yet is clearly visible in the DSD absorption spectrum. The spectra calculated by DSD have not been subjected to any noise reduction procedures and yet the successful resolution of all six genuine peaks in the frequency window is achieved without any difficulty.

In Table 1, we compare the exact parameters used to generate the time signal with those recovered by analysis of the "noisy" signal using DSD. For each of the six signal peaks in the considered window, DSD retrieves the frequency to well within 0.005 Hz of the true value. Note that, for the noiseless signal, DSD retrieves to machine accuracy all of the exact signal parameters listed in Table 1. This comparison gives a guide to the expected level of error when using DSD to analyze experimental ICR time signals embedded in noise of a moderate level.

Next, we discuss the spectral analysis of the experimental ICR time signals for $[C_{59}N]^+$ and $[C_{60}]^+$. These experiments

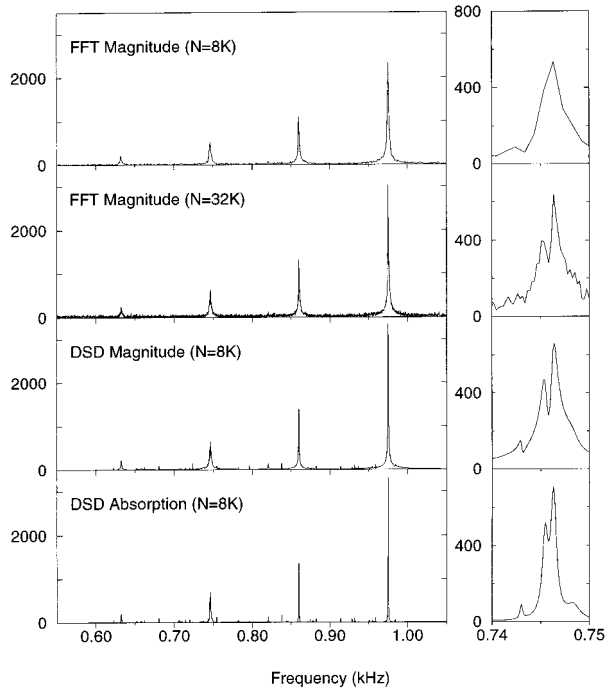

Figure 4. ICR frequency spectra for isotopic fine structure of Milled Wood Lignin (pinoresinol lignin molecular compound). The signal was recorded at the Ångström Laboratory (Uppsala, Sweden) using the collisionally induced dissociation (CID) together with tandem FT-ICR mass spectroscopy. The panels on the right-hand side show magnifications of the isotopic peak (a doublet) located at 0.74−0.75 kHz. With only one-quarter of the full signal length; DSD resolves the whole elemental isotopic composition with the correct relative abundance of the constituents. The left and right peaks on the inserts correspond to isotopes $^{13}C_2$ and ^{34}S, respectively.

were performed at the Department of Chemistry at the University of California at Santa Barbara by the Matrix Assisted Laser Desorption Ionization (MALDI) of admixtures of azafullerene, $(C_{59}N)_2$, and fullerene, C_{60}. The spectra calculated by FFT and DSD are displayed in Figure 3 in order of increasing improvement from top to bottom. As is clear from this figure, to resolve all the six isotope peaks in the selected window, FFT needs the full signal length, $N = 64$ K. However, DSD achieves the same result by using only one-quarter, $N = 16$ K, of the measured time signal. Even with such a signal, which is considerably shorter than the one provided with the full acquisition time, DSD resolves the isotopic admixtures to within a fraction of one kHz (which corresponds to a fraction of one Da on the mass scale). Moreover, with the same short signal, DSD is able to detect the smallest peak of ∼1/10 th of the magnitude of the central largest structure. The DSD results for $N = 16$ K and $N = 64$ K are indistinguishable from each other on the scale of Figure 3.

In Figure 4, we present the results of our third test example concerning the experimental ICR time signal for the so-called "Milled Wood Lignin (MWL)" in its covalent molecular compound—pinoresinol. This experiment has been carried out at the Ångström Laboratory of the University of Uppsala (Sweden), where the sample of MWL was obtained by chemically treating softwood lignin with the help of thioacidolysis and fractionation. Lignin, as the second most abundant organic molecule on Earth, accounts for about 30% of the dry weight in softwood and thus plays an important role in wood and paper chemistry as well as technology. This ICR experiment with the lignin sample was performed with the help of an accompanying technique known as the collisionally induced dissociation (CID).[9] The resulting ICR time signal carries information on isotopic fine structure which provides an insight into the elemental composition of MWL. In the left-hand panels of Figure 4, we plot the corresponding spectra in the frequency region from 0.55 to 1.05 kHz. Analysis of this whole frequency range (which corresponds to approximately one-sixteenth of the total spectral bandwidth) in one run by DSD would result in a generalized eigenvalue problem of dimension 1 K, if the full

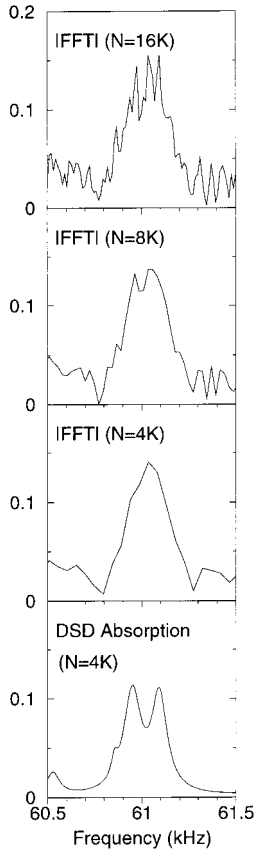

Figure 5. ICR frequency spectra for isotopic fine structure of apotransferrin in the region of a doublet located at 61 kHz. The signal was recorded at the Ångström Laboratory (Uppsala, Sweden). The top three panels show the FFT magnitude spectra obtained using $N = 16$ K, $N = 8$ K, and $N = 4$ K of the measured signal points. The bottom panel depicts the corresponding DSD absorption spectrum obtained utilizing only $N = 4$ K.

TABLE 1: Comparison of Exact and DSD-Determined Parameters for a Synthesized Time Signal Consisting of a Sum of Exponentially Decaying Oscillations, with Known Frequencies, Amplitudes, Phases, and Damping Constants[a]

	frequency (kHz)	damping const (s^{-1})	amplitude	phase (deg)
exact	0.015 870 00	0.100 00	0.150 00	60.000 00
DSD	0.015 866 63	0.065 20	0.114 03	55.418 17
exact	0.015 760 00	0.040 00	0.600 00	45.000 00
DSD	0.015 759 77	0.039 52	0.592 76	45.827 82
exact	0.015 640 00	0.050 00	0.300 00	135.000 00
DSD	0.015 639 68	0.049 66	0.323 28	134.202 04
exact	0.015 585 00	0.040 00	0.400 00	60.000 00
DSD	0.015 585 92	0.037 29	0.359 76	64.271 08
exact	0.015 570 00	0.040 00	0.300 00	10.000 00
DSD	0.015 570 46	0.041 85	0.346 56	11.193 11
exact	0.015 450 00	0.050 00	0.200 00	10.000 00
DSD	0.015 453 13	0.057 86	0.239 68	32.200 09

[a] Prior to processing with DSD, 30% Gaussian distributed random white noise with zero mean was added to the signal. Only those parameters for the six peaks occurring in the frequency range 0.015−0.016 kHz are reported here.

signal length of $N = 32$ K is used. Instead, we further subdivided the range 0.55−1.05 kHz into four overlapping windows, each of width 0.12 kHz. Each small window was analyzed in turn to obtain all the peak parameters over the full frequency interval of interest. Finally, the DSD magnitude and absorption spectra presented in Figure 4 were calculated using eqs 14 and 15, respectively.

The right-hand panels of Figure 4 show magnifications of the spectra in the region of the doublet at 0.74−0.75 kHz. Again, it is evident from this figure that FFT is unable to resolve the doublet when only one-quarter ($N = 8$ K) of the measured time signal is used. The doublet is, however, resolved successfully by using DSD with $N = 8$ K.

It is clear from the above comparison that DSD converges faster than FFT. This in itself might be a useful advantage from a noise reduction viewpoint.[6] The signal usually decays exponentially, whereas some sources of noise often remain relatively constant in time. The result is that, at long times, noise can dominate the signal. Although the noise is preserved in the band-limited decimated signal c_n^{bld} of length N_{D}, by using a shorter signal, DSD automatically works with a less "noisy" signal.

The above point is dramatically demonstrated in our final example, which concerns the isotopic fine structure of apotransferrin. This experimental ICR time signal was also measured at the Ångström Laboratory of the University of Uppsala (Sweden). The apotransferrin sample was purchased commercially from Sigma Aldrich and had a mass of around 77 kDa. It was electrosprayed in a 50:50 methanol:water mixture to which 2% acetic acid was added. In Figure 5, we concentrate on a small region of the corresponding frequency spectrum in the vicinity of a doublet at 61 kHz. The top three panels show the FFT magnitude spectra obtained using $N = 16$ K, $N = 8$ K, and $N = 4$ K. With $N = 4$ K and $N = 8$ K signal points, FFT fails to unambiguously resolve the doublet. However, increasing the signal length to $N = 16$ K does not yield the expected increase in the FFT resolution. In this case, increasing the acquisition time to achieve the required resolving power has resulted in the recording of points where the signal is overwhelmed by noise. The result is a significant deterioration in the quality of the spectrum. Here, the superior frequency resolution of DSD enables the separation of the doublet with $N = 4$ K signal points as shown in the bottom panel of Figure 5.

As we have demonstrated with the above four examples, DSD provides a powerful method for analyzing time signals embedded in noise of moderate levels, such as those typically recorded in ICR, NMR, or FTIR experiments. It is important to note, however, that in the presence of noise, DSD will usually extract some small spectral features in addition to the true signal peaks; typical examples can be seen in the DSD spectra displayed in Figure 2. Of course, these additional peaks should not be interpreted automatically as true signal features. In contrast to the signal peaks, these supplementary spectral features frequently display extreme sensitivity to such parameters as the window size and location or the signal length.[6] As a result, such additional features can usually be identified as noise peaks. For signals embedded in more significant noise levels, it becomes increasingly difficult to distinguish between signal and noise features in the DSD spectra. Of course, it should be noted that this is a problem which also afflicts every other signal processing approach, including the FFT.

In summary, we started the analysis with a synthesized time signal and showed that the known peak parameters $\{\omega_k, d_k\}$ can be obtained very accurately and without difficulty. This model problem is sufficiently realistic in the sense that its 30% noise level should be able to mimic some usual random contaminations in experimental ICR time signals. Then we passed onto the three quite different experimental ICR signals (a fullerene-type cluster, lignin, and apotransferrin) to assess fidelity and overall performance of DSD in comparisons with the FFT. In the case of a fullerene-type cluster analyzed in Figure 3, the DSD achieves an enhanced resolution with fewer signal points relative to FFT. Regarding the lignin molecular compound shown in Figure 4, analysis of the full spectral range of interest with DSD requires more than one sub-window, but the present method still outperforms FFT by using only one-quarter of the full signal length. Finally, we conclude our testings in Figure 5 with the most difficult signal of the very "noisy" sample of apotransferrin for which FFT cannot extract any useful information from the experimental data. By contrast, the DSD is still able to display its superiority by retrieving the doublet from the heavily contaminated background. This is done by the direct run of the DSD algorithm without the application of any noise reduction techniques. Some supplementary "denoising" procedures within the postprocessing stage of the spectral analysis may additionally enhance the capability of DSD beyond the present achievement as has actually been demonstrated successfully in ref 6.

4. Conclusion

A stable, user-friendly, and robust signal processing method named Decimated Signal Diagonalization (DSD) is proposed. This method is specifically designed for all Lorentzian spectra that originate from sums of damped time exponentials with stationary amplitudes. For the purpose of illustration, the DSD is applied to experimental ion cyclotron resonance (ICR) spectroscopy data that are associated with Lorentzian spectra. The DSD is a parameter estimator which exhibits a 2-fold advantage over the most frequently employed spectral estimator, the Fast Fourier Transform (FFT). *First*, DSD determines all the peak parameters (positions, magnitudes, relaxation times, phases, etc.) and then constructs a spectrum in any desired mode. This includes absorption, which has a better resolving power than the corresponding magnitude spectrum. The absorption spectra are easily obtained without any additional experimental effort, as no phase problems exist. *Second*, when a spectrum is not too densely packed with spectral or noise features, remarkably good results can be achieved with a considerably shorter acquisition time than needed by FFT. Although the examples presented here correspond specifically to ICR experiments, DSD can equally well be applied to any arbitrary length, exponentially attenuated time signals corresponding to spectra that are sums of pure Lorentzians such as those measured typically in ICR, NMR, FTIR, etc., experiments.

Acknowledgment. The DOE (Contract No. 53-4815-248), the National Science Foundation (NSF Grant No. PHY-9802534), the donors of the Petroleum Research Fund administered by the American Chemical Society, Stockholm County Council, the Deutsche Forschungsgemeinschaft, and the Deutscher Akademischer Austauschdienst are each acknowledged for partial support of the present research. J.M. thanks H.S.T. and the University of Southern California for their kind hospitality during the initial stage of this work. The authors thank Dr. Jan Axelsson and MSci. M. Palmblad from the Ångström Laboratory's Division of Ion Physics at the University of Uppsala (Sweden) for kindly supplying their time signals for lignin and apotransferrin.

References and Notes

(1) Belkić, Dž.; Dando, P. A.; Taylor, H. S.; Main, J. *Chem. Phys. Lett.* **1999**, *315*, 135−139.

(2) Wall, M. R.; Neuhauser, D. *J. Chem. Phys.* **1995**, *102*, 8011−8022.

(3) Mandelshtam, V. A.; Taylor, H. S. *J. Chem. Phys.* **1997**, *107*, 6756−6769; Mandelshtam, V. A.; Taylor, H. S. *J. Chem. Phys.* **1998**, *109*, 4128 (erratum).

(4) Guan, S.; Marshall, A. G. *Anal. Chem.* **1997**, *69*, 1156−1162.

(5) Shin, S. K.; Han, S.-J. *Int. J. Mass. Spec. Ion Proc.* **1996**, *153*, 87−99. Shin, S. K.; Han, S.-J. *J. Am. Soc. Mass. Spec.* **1997**, *8*, 86−89.

(6) Belkić, Dž.; Dando, P. A.; Main, J.; Taylor, H. S. *J. Chem. Phys.* **2000**, *113*, 6542−6565.

(7) Main, J.; Dando, P. A.; Belkić, Dž.; Taylor, H. S. *J. Phys. A: Math. Gen.* **2000**, *33*, 1247−1263.

(8) NAG Fortran Library, *Numerical Algorithms Group*, 256 Banbury Road, Oxford OX2 7DE, United Kingdom.

(9) Palmblad, M.; Önnerud, H.; Håkansson, K.; Axelsson, J. *Inter. Conf. Am. Soc. Mass. Spectrosc. (Dallas, Texas, USA, 1998)*; CD.